Macromodel Extraction of Gas Damping Effects for Perforated Surfaces with Arbitrarily-Shaped Geometries

Yao-Joe Yang and Cheh-Jia Yu

Department of Mechanical Engineering
National Taiwan University
1 Roosevelt Rd. Sec 4., Taipei, Taiwan, ROC
yjy@ccms.ntu.edu.tw, TEL:+886 2 23646491 FAX:+886 2 23631755

ABSTRACT

In this work, we present an application of an Arnoldi-based model order reduction (MOR) technique on squeezed-film damping (SQFD) effects for arbitrarily-shaped perforated geometries. The compact models generated by this approach not only can be easily inserted into a system-level modeling package for transient and frequency analysis, but also accounts for the effect of flow impedance of each perforation. The simulated results of the reduced models show good agreement with the experimental results. We also demonstrated that this approach is at least 100 times faster than previous works on perforated SQFD damping simulation.

Keywords: damping, model order reduction, squeeze film damping, perforation, perforation flow impedance

INTRODUCTION

Perforations are often used in MEMS devices either to reduce release-etch time or to control squeeze-film damping effects. Modeling of *arbitrarily-shaped* perforated MEMS devices can be extremely complicated. Most work in damping has focused on getting more accurate simulations of the small or large signal gas damping and spring effects [1-6]. However, these studies are not suitable for effectively simulating perforated surfaces because of neglecting the flow impedance of perforation holes. Veijola [7] introduced a special term into the SQFD governing equation, the Reynolds equation, to account for the *total* acoustic impedance effect due to evenly distributed perforations, and derived compact analytically solutions. This approach provides designers compact and efficient SQFD models for perforated devices, but is limited to the cases of rectangular-shaped surfaces (with uniformly -distributed perforations) for which the analytical solutions exist. Yang [8] has developed a flow impedance model with the Reynolds equation, and solved the system using finite-difference method. Although this methodology is applicable for the cases of arbitrary plate-shapes and perforation- configurations, the computational cost is very expensive due to the complexity of meshes. In this work, we employ an Arnoldi-based MOR algorithm [9] to generate low-order models from a Finite element (FEM) or Finite difference (FDM) approximation of the *modified Reynolds equation* that is coupled with pressure leakage due to perforations. The procedure of this approach is shown in Figure 1. Because the model size of the low order system is much small than the original FEM/FDM system, the transient calculation is improved by about two order of magnitude. Also, the frequency analysis can be easily performed using eigen expansion techniques.

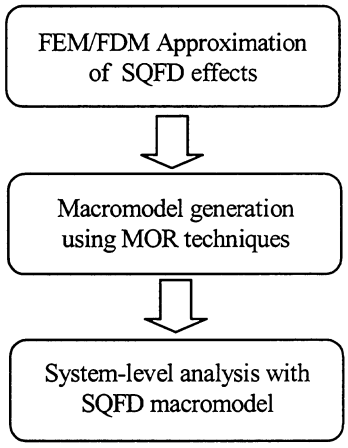

Figure 1 *Procedure of the efficient and accurate air damping modeling for perforated MEMS devices described in this paper*

THEORY

The Arnoldi-based model order reduction (MOR) algorithm known as PRIMA [9], which is commonly used for model reduction of electrical interconnects, is used for model extraction. Our approach is similar to the model reduction approach used in [10]. In [10], model reduction was applied to a linearized form of the fully coupled electro-mechanical-fluid damped system. Here, we focus on the correct modeling of perforation effects, and treat the squeeze film damping separately [11]. The SQFD models are built in the mechanical mode shape basis. Such an approach would allow these models to be readily combined with the mode shape based models in the low order model of the entire system [3]. Additionally, we show that the models can be used for large-signal motion with certain restrictions.

To begin, the linearized Reynolds equation for squeeze film damping from [1] is

$$\frac{h_0}{P_0}\cdot\frac{\partial P}{\partial t}=\frac{h_0^3}{12\mu}\nabla^2 P-\frac{\partial e}{\partial t} \qquad (1)$$

where the variation in plate spacing h is assumed to be small compared to the mean spacing, h_0, given by

$$h = h_0 + e(x,t)$$

with $x \in \Re^2$ and $e << h_0$. The variation in pressure, P, will thus be small compared to ambient,

$$P = P_a + p(x,t)$$

In order to account for the perforation effect, we employ an the modified Reynolds equation that is coupled with pressure leakage due to perforations:

$$\frac{\partial p}{\partial t}=\frac{P_a h^2}{12\mu}\nabla^2 p-\frac{P_a}{h}\cdot\frac{p}{Z}-\frac{P_a}{h}\cdot\frac{dh}{dt} \qquad (2)$$

where p is pressure variation, h is gap thickness, P_a is ambient pressure and μ is viscosity. Note that the derivation of this equation is based on the condition of flow continuity [8]. The second term on the right-hand side of Equation 2 accounts for the acoustic *pressure leakage* due to perforation.

The impedance Z in the equation represents flow impedance for each hole. The value of Z is in fact an analytical form of pipe flow resistance, which can be found in [8].

$$Z=\frac{128\mu L}{\pi D_c^4} \qquad (3)$$

where L is the pipe length, D_c is the diameter of the perforation. The value of Z also depends on the perforation location. Z is infinite at the location where a hole does not exist. In other words, the pressure leakage term is eliminated at the location where a hole does not exist.

Equation (1) can be solved by finite-element or finite-difference analysis for a given $e(x,t)$. Let $f(x)$ be the shape (perhaps mode shape) of the displacement so that $e(x,t) = f(x)\cdot u(t)$. The dynamic system from discretizing (2) by FEM or FDM can be written in a state space form as

$$\begin{aligned}\frac{h_0}{P_0}B\frac{d\mathbf{p}}{dt}&=\frac{h_0^3}{12\mu}A_D\mathbf{p}+A_Z\mathbf{p}+B\mathbf{f}u(t)\\ y&=(B\mathbf{f})^T\mathbf{p}\end{aligned} \qquad (4)$$

where $A_D, A_Z, B \in \Re^{n\times n}$, n is the number of nodal degrees of freedom, $\mathbf{p}$ is the pressure at the nodes, and $\mathbf{f}$ is $f(x)$ evaluated at the node points. y is then the net force projected into the shape defined by $f(x)$.

The matrices A_D and A_Z can be merged into a new single matrix A, as shown in Equation 5.

$$\begin{aligned}\frac{h_0}{P_0}B\frac{d\mathbf{p}}{dt}&=\frac{h_0^3}{12\mu}A\mathbf{p}+B\mathbf{f}u(t)\\ y&=(B\mathbf{f})^T\mathbf{p}\end{aligned} \qquad (5)$$

The dynamic system of (5) is too large to insert directly into a system simulator such as SPICE or SABER. We thus apply PRIMA to generate a low order representation of (5) which still accurately captures the dynamic behavior. To apply the PRIMA algorithm to generate a k-th order model, k orthogonal vectors $\{v_i\} \in \Re^n$ are computed which span the vector space known as Krylov subspace:

$$K_k=\left\{(B\mathbf{f}),A^{-1}B(B\mathbf{f}),\ldots,\left(A^{-1}B\right)^{k-1}(B\mathbf{f})\right\}$$

These vectors can be stably computed via the Arnoldi algorithm [9]. Given the matrix V whose columns are $\{v_i\}$, the reduced order model is

$$\begin{aligned}\frac{h_0}{P_0}\tilde{B}\frac{d\tilde{\mathbf{p}}}{dt}&=\frac{h_0^3}{12\mu}\tilde{A}\tilde{\mathbf{p}}+\tilde{\mathbf{f}}u(t)\\ y&=\tilde{\mathbf{f}}^T\tilde{\mathbf{p}}\end{aligned} \qquad (6)$$

where $\tilde{B}=V^TBV$, $\tilde{A}=V^TAV$, and $\tilde{\mathbf{f}}=V^TB\mathbf{f}$. The attractive properties of such an approach are that the first k Taylor series coefficients of the transfer function of (6) match those of the original model in (2). In addition, the model is guaranteed to be passive. Finally, the method easily extends to a single model with multiple inputs $\{u_1(x),u_2(x),\ldots.\}$ corresponding to multiple mode shapes, $\{\mathbf{f}_1(x),\mathbf{f}_2(x),\ldots.\}$.

As will be seen in the next section, k = 20 is generally adequate for an accurate damping model. This low order model can be inserted directly into a system simulator such as SPICE or SABER. Note that since the vector space spanned by $\{v_i\}$ does not depend on the mean gap, ambient pressure or viscosity, the above model is valid for any choice of those parameters. Going one step further, we can model large signal behavior by letting the mean gap vary with time, $h_0 = h_0(t)$. Such an approach would be valid if $h_0(t)$ varies slowly compared to $u(t)$. In fact, from numerical experiment, we find that replacing h_0 in (2) with $h_0(t) = h_0 + u(t)$ for even large $u(t)$ gives good results.

RESULTS

Figure 2 shows a schematic view of a bulk-micromachined accelerometer [12] whose damping effects are studied in this work. The perforated proof-mass of the device is supported by four flexible tethers. The surface area of proof-mass (under SQFD effects) is 515x515 μm^2. The plate thickness is 10.8 μm, which is also the length L of the flow impedance Z (Equation 3). The configuration of perforations on the proof-mass is shown in Figure 3. The total number of perforations is 36x36. The distance between hole centers is 18 μm, and the size of each hole is 2x2 μm^2.

The results of damping and spring components for a 515x515 μm^2 perforated accelerometer are shown in

Figure 4. The original system has 66564 nodes (i.e., 66564x66564 system matrix), which is too large to be compatible with system-level simulations. In previous works, the damping and spring components can be obtained by solving Equation 1 for different imposed oscillation frequencies. However, the computational time is more than two order of magnitude of the time for solving a suitable reduced model that can be generated by the approach presented in this work [11]. Our results indicate that a reduced macromodel of order 20 (i.e., 20x20 system matrix) gives accurate and converged results.

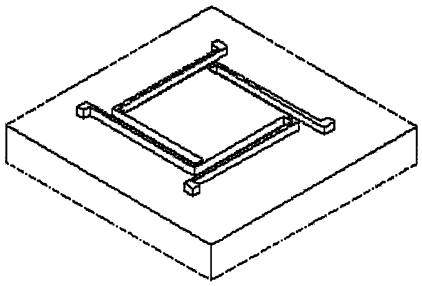

Figure 2 *The schematic of an bulk-micromachined accelerometer. The proof-mass is suspended by four tethers. The dimension of the proof-mass is 515x515 μm^2.*

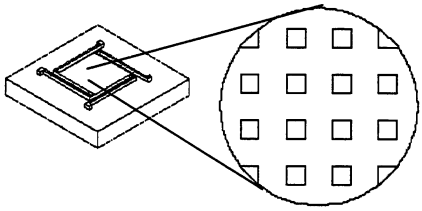

Figure 3 *The configuration of perforations on the proof-mass of the accelerometer shown in Figure 2. The size of the hole is 2x2 μm^2, and the pitch is 18 μm. There are totally 36x36 holes evenly distributed on the proof-mass.*

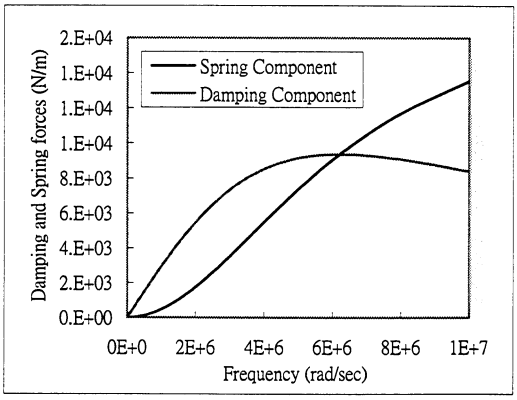

Figure 4 *Spring and damping components of an order-20 macromodel for a 515x515μm^2 perforated accelerometer. The gap is 1μm.*

With the simulated spring and damping components of the perforated SQFD effects, we formulated the dynamic mass-spring-damper system of the accelerometer, as shown in Figure 5. The mass and the mechanical spring are the corresponding to first mode of oscillation (i.e., out-of-plane motion). The *air spring* and *air damping* effects in the schematic are functions of oscillation frequency, as shown in Figure 4. The simulated damping ratio of 5.6 at 10 KHz is very close to the experimental result of about 5 [8,12], as shown in Figure 6. Note that since the perforations effectively released the pressure gradient inside the gap during the oscillation of the proof-mass, the gas compression effect is not obviously at 10 KHz (relatively low frequency). Therefore, the spring effect is negligible in this case. The extracted macromodels can be easily inserted into circuit simulators [9] or system-level simulators such as Saber or Simulink [13]. Figure 7 shows the schematic of a Mass-Spring-SQFD model under Simulink environment. The extracted SQFD macromodel is described as a state-space model of the Simulink. The Simulink transient simulation of the system under a step input voltage is shown in Figure 8. The frequency of the oscillation at the beginning of the curves is the resonance frequency of the device. The figure shows that for the reduced models whose orders are equal to or greater than 20, the results are in good agreement with FDM results.

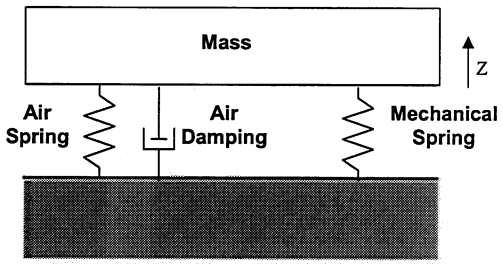

Figure 5 *A Mass-spring-damper schematic of the accelerometer shown in Figure 2. The "Air Spring" and "Air Damping" are frequency-dependent and can be obtained from Figure 4.*

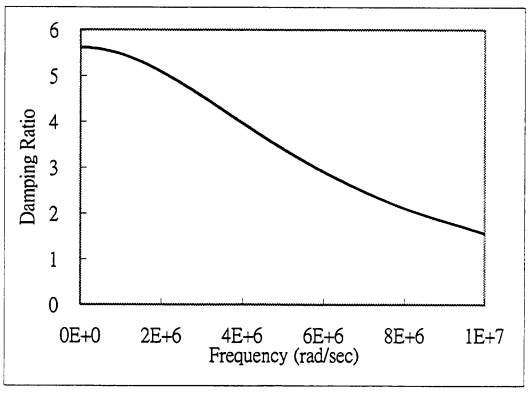

Figure 6 *Damping ratio of the accelerometer. The mechanical spring constant is 4.75 N/m, and the mass is 1.52e-8 kg. The experimental damping ratio at 10 kHz is about 5.*

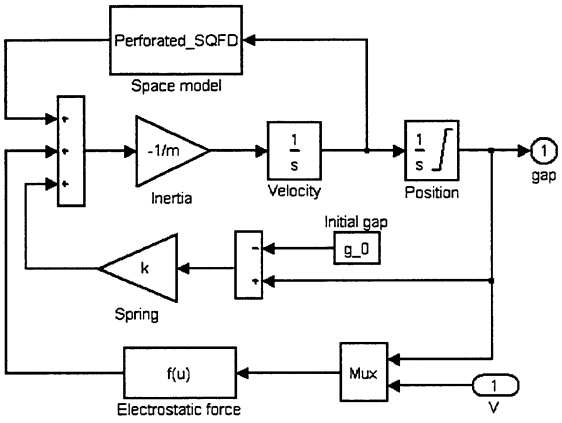

Figure 7 *Schematic of mass-spring-SQFD model of an accelerometer with electrostatic actuator. The extracted SQFD macromodel is described as a state-space model of the Simulink.*

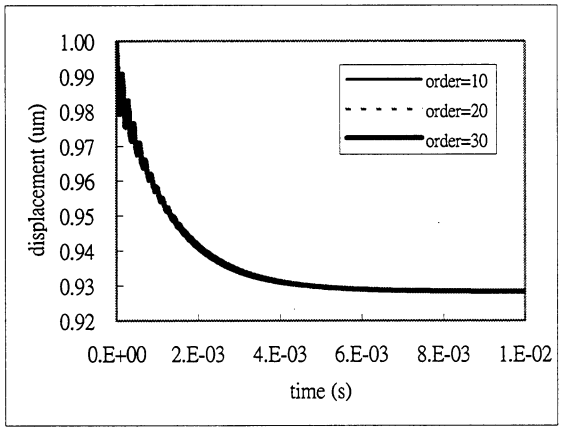

Figure 8 *Transient simulation result of the accelerometer system shown in Figure 2. The applied voltage is 0.5 volt. The ambient pressure is set to 0.001atm so that oscillation will be observed. The curves of order 20 and 30 systems are identical*

CONCLUSION

A new approach to extract frequency-dependent gas damping models for perforated arbitrary geometries of MEMS devices is demonstrated. The Arnoldi-based algorithm is applied for creating a low-order model from the transient FEM/FDM system matrices. The frequency-dependant gas damping and spring effects can be obtained using the low-order models without any computationally intensive transient simulation for wide frequency range. After constructing 3D solid models, more than two order of magnitude reduction in computational time has been demonstrated. Examples of transient analysis and comparison to experimental results are also provided.

ACKNOWLEDGEMENT

This work is funded by the National Science Council (NSC), Taiwan, ROC (contract number NSC 90-2218–E-002-024).

REFERENCES

1. J.J. Blech, " On Isothermal Squeeze Films", *Journal of Lubrication Technology*, Vol. 105, 1983, 615-620.
2. T. Veijola, et. al. "Model for Gas Film Damping in a Silicon Accelerometer" , Trans. 97, pp. 1097-1100
3. Y-J. Yang, et. al., "Effects of Air Damping on the Dynamics of NonUniform Deformations of Microstructures", Trans. 97, 1093-1096
4. M-A. Gretillat, "Electrostatic Polysilicon Microrelays" Ph.D. Thesis, IMT, University of Neuchâtel, Switzerland 1997
5. T. Veijola, "Finite-Difference Large Displacement Gas-Film Model" , Trans. '99, pp1152-1155.
6. M.G da Silva, et. al.,"Gas Damping and Sprng Effects on MEMS Devices with Multiple Perforations and Multiple Gaps", Trans. '99, pp1148-1151.
7. T. Veijola, et. al., "Compact Squeezed-film Damping Model for Perforated Surface", Trans. 2001, pp1506-1509.
8. Y.-J. Yang, Squeeze-film Damping for MEMS, Master Thesis in Electrical Engineering, Massachusetts Institute of Technology, 1998.
9. A. Odabasioglu, el. al., "PRIMA," IEEE Transaction on Computer-Aided Design of Integrated Circuits and Systems, Vol. 17, No. 8, August 1998.
10. F. Wang and J. White, "Automatic Model Order Reduction of a Microdevice using the Arnoldi Approach," ASME IMECE 98, DSC-Vol. 66, pp527-530
11. Y.-J. Yang, et. al. "Modeling Gas Damping and Spring Phenomena In MEMS With Frequency Dependent Macro-Models" IEEE MEMS 2001.
12. C. H.-Y. Hsu, "Silicon Microaccelerometer Fabrication Technologies," Ph.D. Thesis, Massachusetts Institute of Technology, 1997.
13. Matlab/Simulink Userguide, Version 5.0, The MathWorks Inc.,
14. S. D. Senturia, Microsystem Design, Kluwer, 2001.